HHS Public Access

Author manuscript

Dev Biol. Author manuscript; available in PMC 2017 May 01.

Published in final edited form as:

Dev Biol. 2016 May 1; 413(1): 60–69. doi:10.1016/j.ydbio.2016.03.001.

Receptor tyrosine phosphatase CLR-1 acts in skin cells to promote sensory dendrite outgrowth

Xianzhuang Liu[1,2], **Xiangming Wang**[1,4], and **Kang Shen**[1,3,4]

[1]National Laboratory of Biomacromolecules, Institute of Biophysics, Chinese Academy of Sciences, 15 Datun Road, Chaoyang District, Beijing 100101, China.

[2]University of Chinese Academy of Sciences, Beijing 100101, China.

[3]Howard Hughes Medical Institute, Department of Biology, Stanford University, Stanford, California, 94305-5020, USA.

Abstract

Sensory dendrite morphogenesis is directed by intrinsic and extrinsic factors. The extracellular environment plays instructive roles in patterning dendrite growth and branching. However, the molecular mechanism is not well understood. In *Caenorhabditis elegans*, the proprioceptive neuron PVD forms highly branched sensory dendrites adjacent to the hypodermis. We report that receptor tyrosine phosphatase CLR-1 functions in the hypodermis to pattern the PVD dendritic branches. Mutations in *clr-1* lead to loss of quaternary branches, reduced secondary branches and increased ectopic branches. CLR-1 is necessary for the dendrite extension but not for the initial filopodia formation. Its role is dependent on the intracellular phosphatase domain but not the extracellular adhesion domain, indicating that it functions through dephosphorylating downstream factors but not through direct adhesion with neurons. Genetic analysis reveals that *clr-1* also functions in parallel with SAX-7/DMA-1 pathway to control PVD primary dendrite development. We provide evidence of a new environmental factor for PVD dendrite morphogenesis.

Keywords

Receptor tyrosine phosphatase; CLR-1; PVD; dendrite

Introduction

Sensory dendrite development is essential for the neuronal circuit assembly (Arikkath, 2012). Dendrite abnormalities have been implicated in several human neurological and neurodevelopmental diseases such as schizophrenia, Down's syndrome and autistic spectrum disorder (Jan and Jan, 2010). Compared with axons, dendrites are often shorter but highly branched, suggesting that different factors might be required for dendrite development

[4]Correspondence authors: xmwang@moon.ibp.ac.cn, kangshen@stanford.edu.

compared to axon guidance (Jan and Jan, 2010). Intrinsic factors, including cell surface receptors, downstream signal transduction factors, transcription factors, and cytoskeletal modulators have been reported to function in dendrite morphogenesis (Dong et al., 2015; Puram and Bonni, 2013). Several recent studies in *C. elegans* and *Drosophila* have begun to reveal the extracellular signals that pattern sensory dendrites (Dong et al., 2013; Liang et al., 2015; Salzberg et al., 2013). For example, integrin mediated signaling critically regulates the position of *Drosophila* sensory dendrite in the epidermis (Han et al., 2012; Kim et al., 2012).

In *C. elegans,* PVD and FLP are two highly branched mechano-sensory neurons, enveloping the body and head region, respectively (Albeg et al., 2011). PVD responds to harsh mechanical stimuli and cold temperature (Chatzigeorgiou et al., 2010; Way and Chalfie, 1989), and may have a role in proprioception as ablation of PVD leads to defective body posture (Albeg et al., 2011). A pair of PVDs is born at L2 stage with somas at the lateral midline underneath the hypodermal cells on each side of the worm. It elaborates a series of perpendicularly oriented dendritic branches at stereotyped positions. The 1° dendrites grow from the cell body in the anterior and posterior directions, and then the 2°, 3° and 4° branches grow from the "mother" branches to form candelabra like units called "menorah". The 4° branches develop exclusively between muscles and hypodermal cells, and exhibit regular spacing (Fig.1A).

Several intrinsic factors, including the membrane receptor DMA-1 (Liu and Shen, 2012), transcription factors MEC-3, AHR-1, and ZAG-1 (Smith et al., 2013), the intracellular trafficking component BICD-1 (Aguirre-Chen et al., 2011), the proprotein convertase KPC-1/furin (Salzberg et al., 2014), the unfolded protein response pathway (Wei et al., 2015), and the claudin-like membrane protein HPO-30 (Smith et al., 2013), function cell autonomously in PVD dendrite development. For extrinsic factors, hypodermal expressed SAX-7 and MNR-1 form a tripartite ligand-receptor complex with neuronal DMA-1 to instruct PVD 3° and 4° dendrite morphogenesis (Dong et al., 2013; Liang et al., 2015; Salzberg et al., 2013). On the hypodermal cell surface, the SAX-7/L1CAM forms regular stripe pattern, which instructs the growth of 4° dendrites. The regular SAX-7 stripes are established by the hemi-desmosome stripes between the repeated muscle sarcomeres and the hypodermis (Liang et al., 2015). It is not known if other hypodermal derived factors, except SAX-7 and MNR-1, are required for the growth of PVD dendrite in a non-autonomous manner.

Protein tyrosine phosphatases play pivotal roles in many cellular processes such as cell division, differentiation and neuron development (Johnson and Van Vactor, 2003; Tonks, 2006). In *C. elegans*, *clr-1* encodes a receptor tyrosine phosphatase that negatively regulates the FGF receptor signaling pathway (Kokel et al., 1998). It also plays important roles in axon guidance through inhibiting netrin-mediated axon attraction (Chang et al., 2004), while its function in dendrite development is not known. Here, we showed that CLR-1 functions in the hypodermis to promote PVD dendrite growth by supporting the continuous dendrite extension after the initial filopodia formation. CLR-1's function is dependent on the phosphatase activity but not the extracellular adhesion domain. CLR-1 also promotes the 1° dendrite development in parallel with the SAX-7/MNR-1 pathway.

Results

clr-1 is required for the development of PVD 4° dendritic arbors

From a candidate screen for mutants affecting PVD dendrite development, we found that PVD 4° dendritic arbors were greatly reduced in a temperature-sensitive mutant *clr-1*(*e1745ts*) when shifting the worms from 15°C to 25°C (see temperature shift assay in materials and methods) (Fig.1B, D and H). We also examined *e2530*, a null allele of *clr-1*, and found similar phenotypes as in *e1745* (Fig.1C, H), suggesting that *e1745* is null or strong allele at the restrictive temperature. *clr-1*(*e1745ts*) mutant also showed reduced number of menorah (Fig.1D, I), and formed many ectopic branches from the 1° and 2° dendrites (Fig.1D, J). To exclude the possibility that restrictive temperature (25°C) would cause PVD dendrite phenotypes, we shifted the wild type strain N2 using the same assay, and no PVD dendrite abnormalities were observed (Fig.1B, H-J). To verify that the PVD phenotype was caused by *clr-1*(*e1745ts*), we injected a fosmid containing the *clr-1* genomic locus into *clr-1*(*e1745ts*) mutant. All three aspects of PVD dendrite phenotypes were fully rescued by this transgene (Fig.1E, H-J), indicating that the *clr-1*(*e1745ts*) mutation is responsible for the PVD dendrite phenotypes.

It is reported that CLR-1 negatively regulates the FGFR receptor signaling pathway (Kokel et al., 1998). To test if FGFR receptor signaling is required for PVD morphogenesis, we examined *egl-15* (the sole FGFR encoding gene in *C. elegans*) and *sem-5* (a downstream factor in the FGFR pathway) mutants. Although these mutants showed subtle reduction in menorah number and subtle increase in ectopic branches compared with wild type worm, neither mutants showed reduced 4° branch phenotype, which is the most striking phenotype in the *clr-1* mutants (Fig. S1). Therefore, FGFR receptor signaling pathway might not play essential functions in PVD dendrite morphogenesis.

clr-1 functions in hypodermis to pattern PVD dendrite morphology

To understand where *clr-1* functions, we constructed a transgene with a 4.6kb *clr-1* promoter-driven GFP expression. The GFP signal was expressed in hypodermis, muscle and a subset of neurons, but was not detected in PVD (Fig.1K-M). It suggested *clr-1* functioned outside of PVD to support its dendrite development, although we could not rule out the possibility that *clr-1* was expressed at a very low level in PVD, or that the promoter we used did not contain all the regulatory elements. *clr-1* was highly expressed in muscle and we have reported that muscle sarcomeres are critical in patterning PVD 4° branches (Liang et al., 2015), which raises the possibility that *clr-1* could act in the muscle. To test if the muscle morphology and sarcomere organization are affected by the *clr-1* mutation, we introduced a UNC-97::mCherry transgene into *clr-1*(*e1745ts*) mutants. UNC-97 is a sarcomere component that labels the dense body. We found that the regular periodic structure of UNC-97 was indistinguishable in *clr-1* mutant when compared with wild type animal (Fig. 2A, B), suggesting that *clr-1* might not function in the muscle to modulate PVD 4° dendrites.

To further understand the cellular functions of *clr-1*, we carried out tissue-specific rescue experiment. PVD specific expression of *clr-1* by *ser-2*Prom3 did not rescue this phenotype

(Fig.1F, H-J). However, hypodermis-driven expression of *clr-1* fully rescued all three aspects of the PVD dendrite phenotypes (Fig.1G, H-J). The data indicated that *clr-1* functions in the hypodermis to pattern PVD dendrite morphology in a cell non-autonomous manner.

SAX-7 is the key instructive cue expressed in the hypodermis to pattern the PVD 3° and 4° branches (Dong et al., 2013; Liang et al., 2015; Salzberg et al., 2013). We wondered whether *clr-1* is required to generate the SAX-7 stripe pattern in hypodermis. After shifting *clr-1*(*e1745ts*) mutants to restrictive temperature, the Hyp::SAX-7::YFP stripes were still visible in most hypodermal regions in *clr-1*(*e1745ts*) mutants (Fig.2C-H). Despite the slightly reduced SAX-7 stripe intensity and mild disorganized appearance in some regions, the SAX-7 stripes still exhibited regular spacing, suggesting that *clr-1* may be not required for patterning SAX-7 stripes (Fig.2C-H). These data suggest that the reduction of PVD 4° dendrite phenotype in *clr-1* mutant might not be caused by an abnormal SAX-7 pattern. Furthermore, we also used the *ajm-1*::GFP marker to visualize the whole hypodermis structure, and we found that both wild type and *clr-1* mutants showed similar pattern (Fig.2 I, J), suggesting the hypodermis largely maintained its integrity in *clr-1* mutants. Hence, it is unlikely that the 4° branching defect in *clr-1* mutants is the result of a major defect in the structure or integrity of the hypodermis.

clr-1 is required for PVD 4° dendrite extension but not for filopodia formation

In *clr-1*(*e1745ts*) mutant, PVD 4° dendrite numbers were greatly reduced. There are two possibilities for this defect: the first is that PVD 4° dendrite could not initiate from the tertiary branch, and the second is that PVD 4° dendrite could not further extend and stabilize after initial filopodia formation. To distinguish these two possibilities, we took time-lapse movies of developing *clr-1*(*e1745ts*) mutants and wild type controls. In wild type animals, 4° filopodia initiated from 3° branch and continued to extend (Fig.3A, D, E). The development of 4° branches is a dynamic process with intermittent growth and retraction phases. After the 4° dendrites reached its full length, they were generally stabilized (movie1). In *clr-1*(*e1745ts*) mutants, short 4° filopodia still emerge from 3° dendrite, however, the filopodia do not further extend and stabilize to produce mature 4° dendrites (Fig.3B, D, E and movie2). In addition, the position of filopodia in the *clr-1* mutants are normal, supporting the notion that the SAX-7 mediated patterning for 4° dendrites is largely normal.

SAX-7 is the key instructive cue expressed in the hypodermis to pattern the PVD 4° branches (Liang et al., 2015), we would like to know if SAX-7 is required for the generation of 4° dendritic filopodia. We examined an animal that the SAX-7 stripes were eliminated from the 4° dendrites region, but still exist in 3° dendrites region. To generate these worms, we expressed SAX-7 in the PLM and ALM neurites, which closely associate with the 3° dendrite of PVD in *sax-7*(*nj48*) mutant (Dong et al., 2013). We found that almost no 4° dendritic filopodia could initiate from the rescued 3° dendrites (Fig.3C, D, E and movie3), indicating that the SAX-7 stripes are required for 4° dendritic filopodia formation.

Next, we asked when *clr-1* exerted its function in hypodermis. We shifted the temperature sensitive allele of *clr-1* from 15°C to 25°C at L2, L3, L4, and young adult stage in separate experiments. Temperature shift at the L2, L3 and L4 stage resulted in dramatic defects in PVD morphology, suggesting that *clr-1*'s function is required during the outgrowth phase of

PVD development. Interestingly, we found that even shifting in adult stage caused some subtle but detectable phenotypes, indicating that there are minor maintenance functions of *clr-1* too (Fig3. F-M).

The function of CLR-1 in patterning PVD 4° dendrites is dependent on its phosphatase domain

CLR-1 encodes a trans-membrane receptor phosphatase with extracellular Ig and FNIII domains as well as two intracellular phosphatase domains (D1 and D2) (Fig.1A). To understand which domains are required for PVD dendrite development, we performed structure-function analyses by constructing partial deletion mutant CLR-1 forms lacking specific domains. Deletion constructs were then introduced into the *clr-1*(*e1745ts*) and tested for their ability to rescue the mutant phenotypes. From such analyses, neither ΔIg nor ΔFNIII was required for PVD dendrites because respective truncation construct rescued all aspects of the *clr-1*(*e1745ts*) phenotypes (Fig.4E, F, J-L). However, a truncated construct (ΔD1), lacking the intracellular membrane-proximal phosphatase domain (D1), could not rescue *clr-1*(*e1745ts*) phenotypes (Fig.4G, J-L). Similarly, the truncated construct, deleting membrane-distal phosphatase domain (ΔD2), only partially rescued the *clr-1*(*e1745ts*) phenotype (Fig.4H, J-L), consistent with the report that phosphatase D1 is essential for CLR-1 phosphatase activity and D2 might function in modulating the function of D1 (Kokel et al., 1998). To further test if the phosphatase activity of the D1 domain is required, we engineered a point mutation in D1 domain, C1013G, which specifically disrupts the enzymatic activity (Kokel et al., 1998). This mutant could not rescue *clr-1*(*e1745ts*) phenotype (Fig.4I, J-L), indicating that the intracellular phosphatase activity, but not the extracellular adhesion domain, is essential for CLR-1 in pattering PVD dendrite.

clr-1 functions redundantly with SAX-7/MNR-1 pathway to control PVD 1° dendrite formation

Hypodermal SAX-7 and MNR-1 form tripartite ligand-receptor complex with dendritic surface receptor DMA-1 to instruct 3° and 4° dendrites development (Dong et al., 2013; Liang et al., 2015; Salzberg et al., 2013). To understand the genetic relationship between CLR-1 and SAX-7/MNR-1 pathway, we constructed double mutants between *clr-1*(*e1745ts*) and *sax-7*(*nj48*), *mnr-1*(*wy758*), *dma-1*(*wy686*). In the double mutants, the length of the primary dendrites was greatly reduced when comparing with single mutant (Fig.5D-F, G). Surprisingly, *clr-1*(*e1745ts*) alone did not affect the length of primary dendrites (Fig.5G). The result suggested that *clr-1* functions in parallel with *sax-7*/*mnr-1* pathway to control primary dendrites development.

To understand which domain of CLR-1 is responsible for primary dendrite development, we performed domain analysis using the same constructs mentioned above. The data showed that the extracellular domain deletion constructs could rescue 1° dendrite phenotype in the double mutants (Fig.6E, F, J). However, intracellular phosphatase D1 domain deletion could not rescue the 1° phenotype (Fig.6G, J). Taken together, CLR-1 intracellular phosphatase activity is essential for both 1° and 4° dendrite development.

Discussion

We reported a receptor tyrosine phosphatase CLR-1 acting non-autonomously to control PVD dendrite morphogenesis. In *clr-1*(*e1745ts*) mutants, PVD 4° dendrite number was greatly reduced and a wild type *clr-1* genomic fragment fully rescued the PVD phenotypes. A transcriptional fusion of P*clr-1::*GFP was not detected in PVD, and PVD specific expression of CLR-1 could not rescue the PVD dendrite phenotypes, suggestive of the non-autonomous function of *clr-1*. Indeed, *clr-1* was expressed in the hypodermis and hypodermis expression of *clr-1* fully rescued the PVD phenotypes, indicative of the non-autonomous function of *clr-1*. It has been reported that CLR-1 acts cell-autonomously in AVM to inhibit UNC-40 activity (Chang et al., 2004). These results suggest that the mechanisms of *clr-1* in AVM axon guidance and PVD dendrite development might be different.

CLR-1 contains an extracellular region and two intracellular phosphatase domains. The extracellular Ig domain and FNIII domains most likely form adhesion interactions with other cell adhesion proteins or ligands. Considering the *clr-1* mutant phenotype, we suspected that CLR-1 might function as an adhesion molecule on the hypodermis to promote dendrite growth similar to SAX-7. However, our structure function analyses showed that the Ig or FNIII domains were not required for PVD morphology, suggesting that the CLR-1 does not function as an adhesion molecule. It is reported that the membrane-proximal phosphatase domain (D1) is essential for *clr-1* function *in vivo*, and the membrane-distal phosphatase domain (D2) is catalytically inactive (Kokel et al., 1998). Our domain analysis data also support this idea. Therefore, we hypothesize that CLR-1 dephosphorylates unidentified cytosolic factors in the hypodermis, which is required to promote dendrite formation.

During PVD development, dendritic filopodia form, extend and stabilize to become mature dendrite. With time-lapse movies, we showed that the SAX-7 stripes are required for filopodia initiation. Interestingly, in *clr-1*(*e1745ts*) mutant, the 4° filopodia still initiate from the 3° dendrites but cannot further extend or be maintained to form mature 4° dendrites. Therefore, hypodermal SAX-7 functions as guidance cue for 4° dendrites initiation and hypodermal CLR-1 is responsible for a signal that promotes the growth and maintenance of dendritic filopodia.

While the molecular mechanisms of menorah formation have been partially elucidated, little is known about the mechanisms that mediate primary dendrite extension. We show that *clr-1* also functions to promote PVD primary dendrite extension in a redundant manner with the SAX-7/MNR-1/DMA-1 pathway. Although *clr-1*(*e1745ts*) mutant alone did not show primary dendrite extension phenotype, *clr-1*(*e1745ts*) significantly enhanced the primary dendrite truncation phenotype of *sax-7*(*nj48*), *dma-1*(*wy686*), or *mnr-1*(*wy758*). The primary dendrite function of *clr-1* is also dependent on its intracellular D1 domain but not the extracellular domain, suggesting CLR-1 does not form adhesion with PVD primary dendrites.

Receptor protein tyrosine phosphatases (RPTR) have been shown functioning in axon outgrowth, guidance, and synaptogenesis in cell autonomously in the neurons (Bixby, 2000;

Johnson and Van Vactor, 2003). Our results suggest that CLR-1 can also function in non-neuronal cells to regulate the sensory dendrite development.

Materials and methods

C. elegans strains and genetics

N2 was used as the wild type strain and animals were cultured at 20°C(*clr-1*(*e1745ts*) mutant and control worms were cultured at 15°C then shifted to 25°C for phenotype analysis) on the *Escherichia coli* OP50 seeded nematode growth medium plates according to a standard method (Brenner, 1974). Standard cloning procedure of Clontech In-Fusion PCR Cloning System was used. A 4.6kb genomic DNA upstream *clr-1* start codon was cloned to the pPD95.77 vector to construct the P*clr-1*::GFP plasmid. PCR products were polymerized by Phusion DNA polymerase (New England Biolabs) or TransStart FastPfu DNA Polymerase (Transgen Biotech). All the strains and plasmids used are listed in Table S1 and S2.

Temperature shift assay (TSA)

clr-1(*e1745ts*) is a temperature sensitive allele and PVDs start to grow dendritic arbors from L2 stage. For the temperature shift assay, *clr-1*(*e1745ts*) single or double mutants and the control worms were cultured at 15°C (permissive temperature). Then animals were shifted to 25 °C (restrictive temperature) at various stages of development. The animals were then allowed to develop in 25°C until adult stage for quantification.

Quantification and statistics

For branches and primary dendrite length quantification, *clr-1*(*e1745ts*) animals were shifted to 25°C. Young adult stage animals were imaged under 40X or 100X objective on an Axio Imager M2 microscope (Carl Zeiss). For the quantification of 4° branch initiation, time lapse images of 4° branches were acquired every 5 min for 2h for wild type and *clr-1* mutants, every 3min for 72min for the *sax-7(nj48); Pmec-17::sax-7s* strain. For the 4° branch outgrowth, we measured the net outgrowth of 4° branch between the start (0 min) and the final time point (120min). We compared each image with the preceding time point in the same series. De novo filopodia formation events were identified. Statistics analysis was performed using either ANOVA followed by a posthoc test, Student's t test or Chi-square test for multiple samples.

Fluorescent imaging and time-lapse imaging

After temperature shifts, adult animals were immobilized with 1mg/ml levamisole in M9 buffer and transferred to a small glass slide or dish, then covered by a 3% (w/v) agar pad. Images were acquired using a 40X or 100X objective on a Zeiss Axio Observer Z1 microscope equipped with an electron-multiplying charge-coupled device camera (Andor), a spinning-disk confocal scan head (Yokogawa CSU-X1 Spinning Disk Unit), and the 488- and 561 nm lines of a Sapphire CW CDRH USB Laser System. To detect 4° dendrite initiation and growth, synchronized late L1 worms (cultured at 15°C) were shifted to 25°C and cultured for 20-24h (about early L4 stage). Then, animals with few 4° branches were chosen and GFP image near the PVD cell body were acquired every 5 min at 25°C. The time lapses recordings typically last for 3 hours.

Supplementary Material

Refer to Web version on PubMed Central for supplementary material.

Acknowledgements

We are grateful to the *Caenorhabditis* Genetics Center and Dr. G.S. Ou for strains. This work was supported by the National Basic Research Program of China (2013CB910103), the Howard Hughes Medical Institute and NINDS (1R01NS082208) to K. Shen, and a grant from the NSFC (31201048, 31571061, 31428009) to X.M. Wang and K. Shen, and the CAS/SAFEA International Partnership Program for Creative Research Teams to K. Shen, and the grant of the Youth Innovation Promotion Association of Chinese Academy of Sciences to X.M. Wang.

References

Aguirre-Chen C, Bulow HE, Kaprielian Z. C. elegans bicd-1, homolog of the Drosophila dynein accessory factor Bicaudal D, regulates the branching of PVD sensory neuron dendrites. Development (Cambridge, England). 2011; 138:507–518.

Albeg A, Smith CJ, Chatzigeorgiou M, Feitelson DG, Hall DH, Schafer WR, Miller DM 3rd, Treinin M. C. elegans multi-dendritic sensory neurons: morphology and function. Molecular and cellular neurosciences. 2011; 46:308–317. [PubMed: 20971193]

Arikkath J. Molecular mechanisms of dendrite morphogenesis. Frontiers in cellular neuroscience. 2012; 6:61. [PubMed: 23293584]

Bixby JL. Receptor tyrosine phosphatases in axon growth and guidance. Neuroreport. 2000; 11:R5–10. [PubMed: 10923644]

Chang C, Yu TW, Bargmann CI, Tessier-Lavigne M. Inhibition of netrin-mediated axon attraction by a receptor protein tyrosine phosphatase. Science. 2004; 305:103–106. [PubMed: 15232111]

Chatzigeorgiou M, Yoo S, Watson JD, Lee WH, Spencer WC, Kindt KS, Hwang SW, Miller DM 3rd, Treinin M, Driscoll M, Schafer WR. Specific roles for DEG/ENaC and TRP channels in touch and thermosensation in C. elegans nociceptors. Nature neuroscience. 2010; 13:861–868. [PubMed: 20512132]

Dong X, Liu OW, Howell AS, Shen K. An extracellular adhesion molecule complex patterns dendritic branching and morphogenesis. Cell. 2013; 155:296–307. [PubMed: 24120131]

Dong X, Shen K, Bulow HE. Intrinsic and extrinsic mechanisms of dendritic morphogenesis. Annual review of physiology. 2015; 77:271–300.

Han C, Wang D, Soba P, Zhu S, Lin X, Jan LY, Jan YN. Integrins regulate repulsion-mediated dendritic patterning of drosophila sensory neurons by restricting dendrites in a 2D space. Neuron. 2012; 73:64–78. [PubMed: 22243747]

Jan YN, Jan LY. Branching out: mechanisms of dendritic arborization. Nature reviews. Neuroscience. 2010; 11:316–328. [PubMed: 20404840]

Johnson KG, Van Vactor D. Receptor protein tyrosine phosphatases in nervous system development. Physiological reviews. 2003; 83:1–24. [PubMed: 12506125]

Kim ME, Shrestha BR, Blazeski R, Mason CA, Grueber WB. Integrins establish dendrite-substrate relationships that promote dendritic self-avoidance and patterning in drosophila sensory neurons. Neuron. 2012; 73:79–91. [PubMed: 22243748]

Kokel M, Borland CZ, DeLong L, Horvitz HR, Stern MJ. clr-1 encodes a receptor tyrosine phosphatase that negatively regulates an FGF receptor signaling pathway in Caenorhabditis elegans. Genes & development. 1998; 12:1425–1437. [PubMed: 9585503]

Liang X, Dong X, Moerman DG, Shen K, Wang X. Sarcomeres Pattern Proprioceptive Sensory Dendritic Endings through UNC-52/Perlecan in C. elegans. Developmental cell. 2015; 33:388–400. [PubMed: 25982673]

Liu OW, Shen K. The transmembrane LRR protein DMA-1 promotes dendrite branching and growth in C. elegans. Nature neuroscience. 2012; 15:57–63. [PubMed: 22138642]

Puram SV, Bonni A. Cell-intrinsic drivers of dendrite morphogenesis. Development (Cambridge, England). 2013; 140:4657–4671.

Salzberg Y, Diaz-Balzac CA, Ramirez-Suarez NJ, Attreed M, Tecle E, Desbois M, Kaprielian Z, Bulow HE. Skin-derived cues control arborization of sensory dendrites in Caenorhabditis elegans. Cell. 2013; 155:308–320. [PubMed: 24120132]

Salzberg Y, Ramirez-Suarez NJ, Bulow HE. The proprotein convertase KPC-1/furin controls branching and self-avoidance of sensory dendrites in Caenorhabditis elegans. PLoS genetics. 2014; 10:e1004657. [PubMed: 25232734]

Smith CJ, O'Brien T, Chatzigeorgiou M, Spencer WC, Feingold-Link E, Husson SJ, Hori S, Mitani S, Gottschalk A, Schafer WR, Miller DM 3rd. Sensory neuron fates are distinguished by a transcriptional switch that regulates dendrite branch stabilization. Neuron. 2013; 79:266–280. [PubMed: 23889932]

Tonks NK. Protein tyrosine phosphatases: from genes, to function, to disease. Nature reviews. Molecular cell biology. 2006; 7:833–846. [PubMed: 17057753]

Way JC, Chalfie M. The mec-3 gene of Caenorhabditis elegans requires its own product for maintained expression and is expressed in three neuronal cell types. Genes & development. 1989; 3:1823–1833. [PubMed: 2576011]

Wei X, Howell AS, Dong X, Taylor CA, Cooper RC, Zhang J, Zou W, Sherwood DR, Shen K. The unfolded protein response is required for dendrite morphogenesis. eLife. 2015; 4:e06963. [PubMed: 26052671]

HIGHLIGHTS

1. Receptor tyrosine phosphatase CLR-1 functions in the hypodermis to pattern the PVD dendritic branches.
2. CLR-1 is necessary for the dendrite extension but not for the initial filopodia formation.
3. CLR-1's function is dependent on the intracellular phosphatase domain but not the extracellular adhesion domain.
4. *clr-1* functions in parallel with SAX-7/DMA-1 pathway to control PVD primary dendrite development.

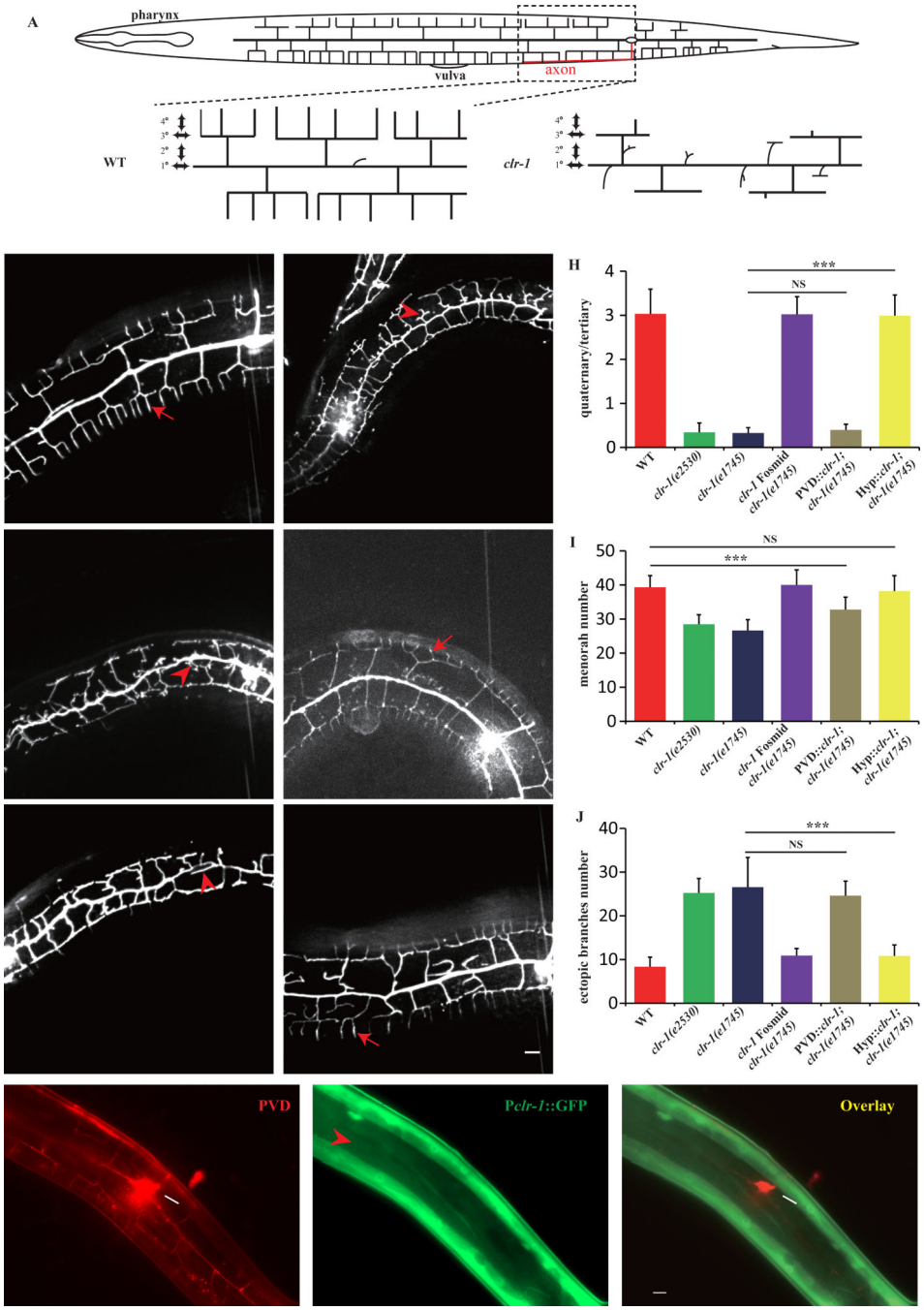

Fig. 1. *clr-1* functions cell non-autonomously in hypodermis to pattern PVD 4° dendrite branches

A) Schematic drawing of the highly branched PVD dendrite in *C. elegans*. B–G) Confocal images of young adult animals expressing *ser-2*Prom3::GFP (all the animals were performed temperature shift assay except for *clr-1*(*e2530*)). Red arrows mark the quaternary dendrites and red arrowheads show the ectopic branches. Scale bar is 10μm. H) Quantification of PVD 4° branch phenotype in wild type, *clr-1*(*e1745*), *clr-1*(*e2530*), fosmid rescue and tissue-specific rescue strains. Y-axis is the average ratio of the number of 4° branches / the number of 3° branches. I) Quantification of number of PVD menorah in wild type, *clr-1*(*e1745*),

clr-1(*e2530*), fosmid rescue and tissue-specific rescue strains. J) Quantification of the number of ectopic branches in wild type, *clr-1*(*e1745*), *clr-1*(*e2530*), fosmid rescue and tissue-specific rescue strains. Ectopic branches were identified as short branches ectopically extended from primary and secondary branches. Error bars, SEM. NS means not significant, ***$p < 0.001$ using ANOVA followed by a posthoc test. $n>30$ for each genotype. K-M) fluorescence images of PVD::mCherry and P*clr-1*::GFP. White arrow marks the cell body and red arrowhead shows hypodermal region. Scale bar is 10μm.

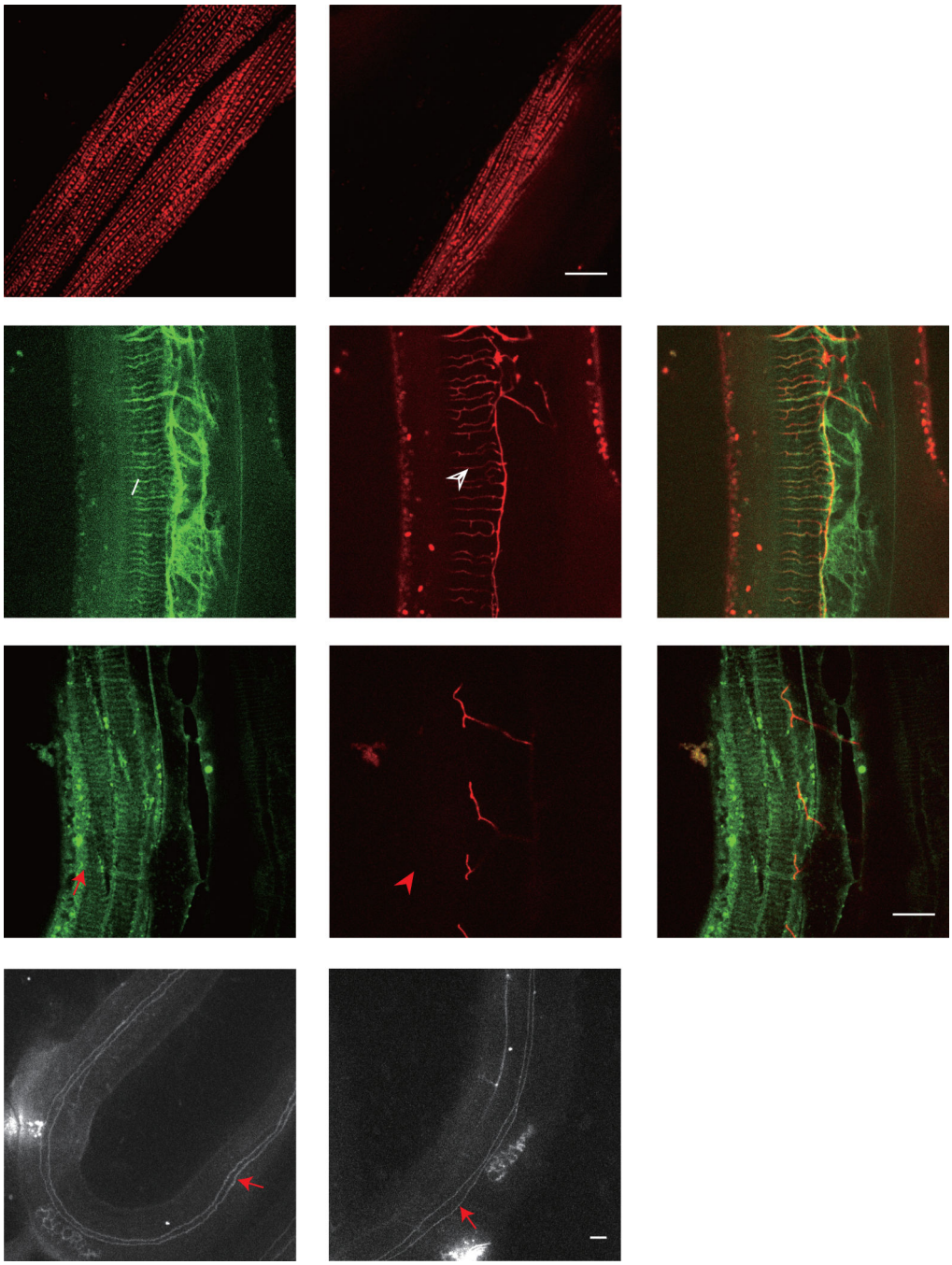

Fig. 2. Reduction of PVD 4° branches in *clr-1* mutant is not caused by SAX-7/DMA-1 pathway or muscle and hypodermal integrity defects

A-B) Confocal images of young adult animals expressing UNC-97::mCherry in muscles in wild type and *clr-1*(*e1745*) mutant, respectively. C-H) Confocal images of young adult animals expressing P*dpy-7*::SAX-7s::GFP in hypodermis and PVD::mCherry in wild type and *clr-1*(*e1745ts*) mutant, respectively. The white arrow marks the SAX-7 stripes and the white arrowhead points to the quaternary dendrites. The red arrow marks the SAX-7 stripes and the red arrowhead points to the same region where no PVD 4° branches form. I-J) Confocal images of young adult animals expressing AJM-1::GFP in wild type and

clr-1(*e1745ts*) mutant, respectively. Red arrows show the fused seam cell boundary with hypodermal cell. Scale bar is 10μm.

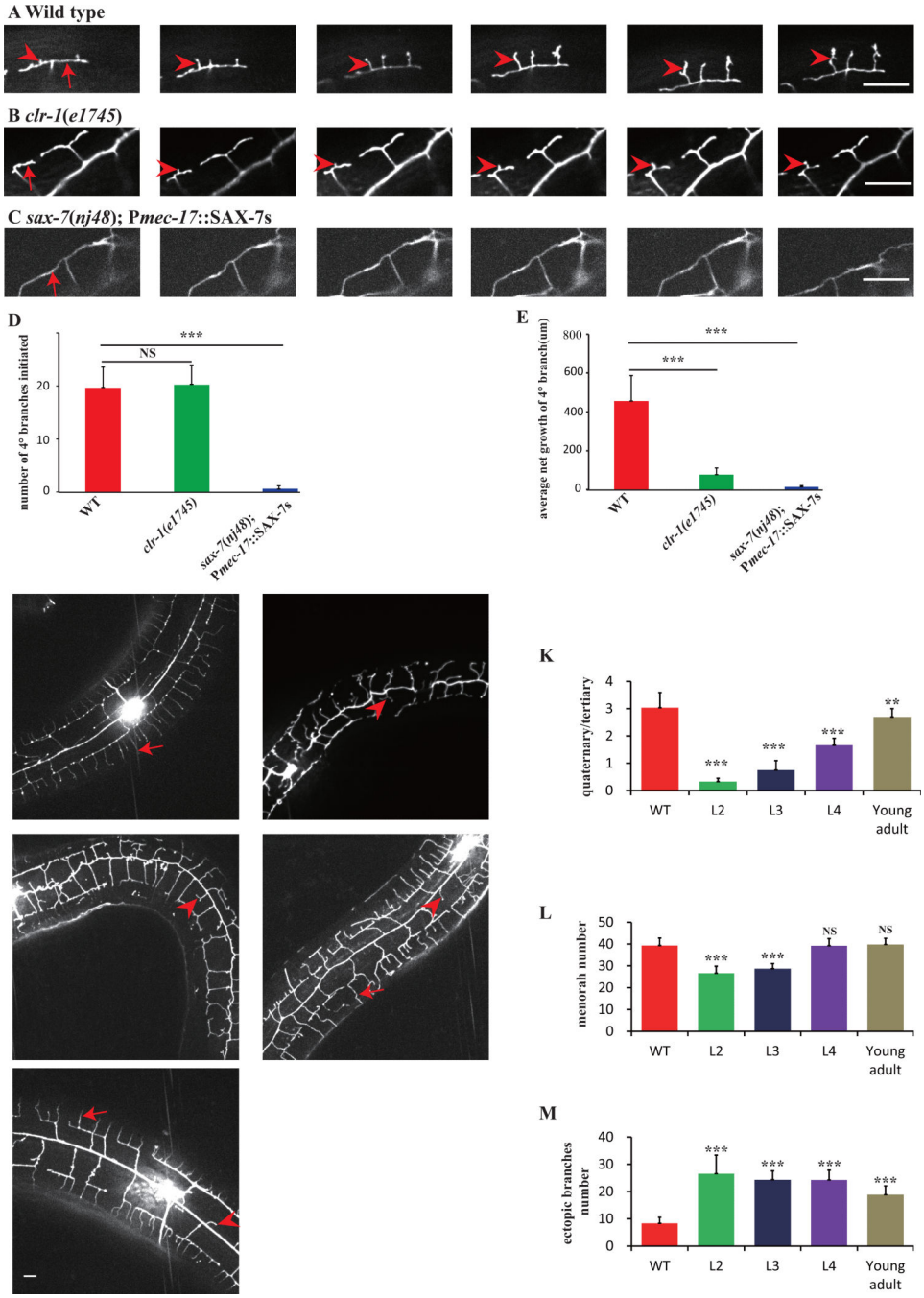

Fig. 3. Time-lapse imaging analyses of 4° branches development

A-C) Still images of time-lapse movies obtained from a wild type (upper panel), a *clr-1*(*e1745ts*) mutant (middle panel), and a *sax-7*(*nj48*); P*mec-17*::SAX-7s animal (lower panel). Numbers on each picture represent time (minutes) when the image was taken. Red arrows mark the 3° branches and red arrowheads indicate the growing 4° branches. Scale bar is 10μm. D) Quantification of the number of 4° branches initiation. E) Quantification of 4° branches net growth in 2h in a visual filed near the cell body. Error bars, SEM. NS means not significant, ***p < 0.001 using ANOVA followed by a posthoc test. n>9 for each

genotype. F-J) Confocal images of wild type or *clr-1*(*e1745ts*) young adult animals shifted from 15°C to 25°C at L2, L3, L4, young adult stage. K) Quantification of PVD 4° branches phenotype in wild type, and *clr-1*(*e1745*) shifted at L2, L3, L4, young adult stage. Y-axis is the average ratio of the number of 4° branches/the number of 3° branches. I) Quantification of the number of menorah in wild type and *clr-1*(*e1745*) shifted at L2, L3, L4, young adult stage. J) Quantification of PVD ectopic branches in wild type and *clr-1*(*e1745*) shifted at L2, L3, L4, young adult stage. Error bars, SEM. NS means not significant, ***p < 0.001 and **p < 0.01 using ANOVA followed by a posthoc test. n>30 for each genotype.

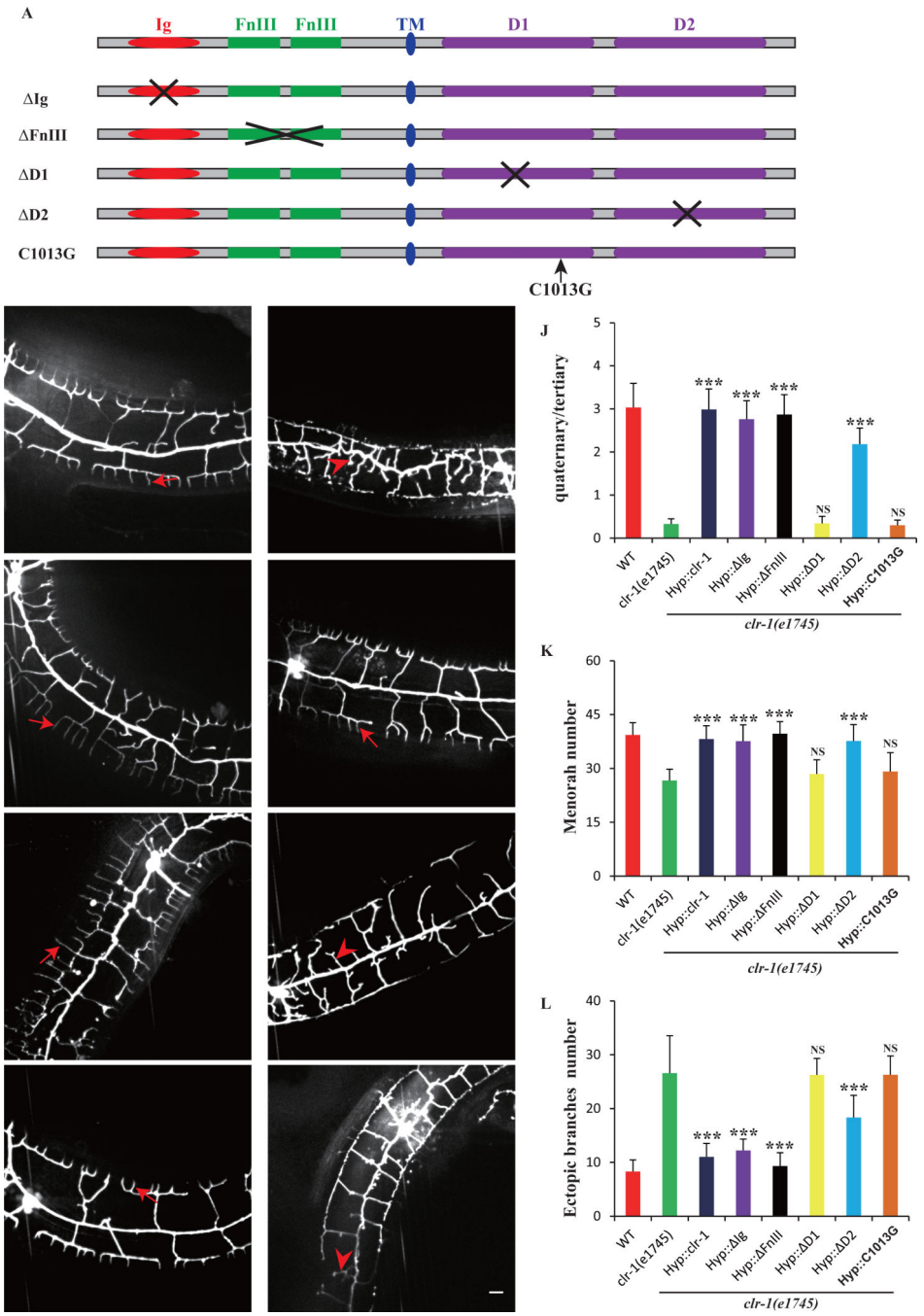

Fig. 4. Intracellular phosphatase D1 domain is essential for *clr-1*'s function in PVD dendrite morphogenesis

A) Schematic picture of CLR-1 protein domain and various deletion mutants. B-I) Confocal images of young adult *clr-1*(*e1745*) and various rescue strains in *ser-2*Prom3::GFP. Red arrows indicate the quaternary dendrites and red arrowheads indicate the ectopic branches. Scale bar is 10μm. J) Quantification of PVD 4° branch phenotype in *clr-1*(*e1745ts*) and various transgenic lines expressing different truncation constructs. Y-axis is the average ratio of the number of 4° branches / the number of 3° branches. K) Quantification of PVD menorah number in *clr-1*(*e1745ts*) and strains expressing various truncation constructs. L)

Quantification of the number of ectopic branches in *clr-1*(*e1745*) and strains expressing various truncation constructs. Error bars, SEM. NS means not significant, ***p < 0.001 using ANOVA followed by a posthoc test. n>30 for each genotype.

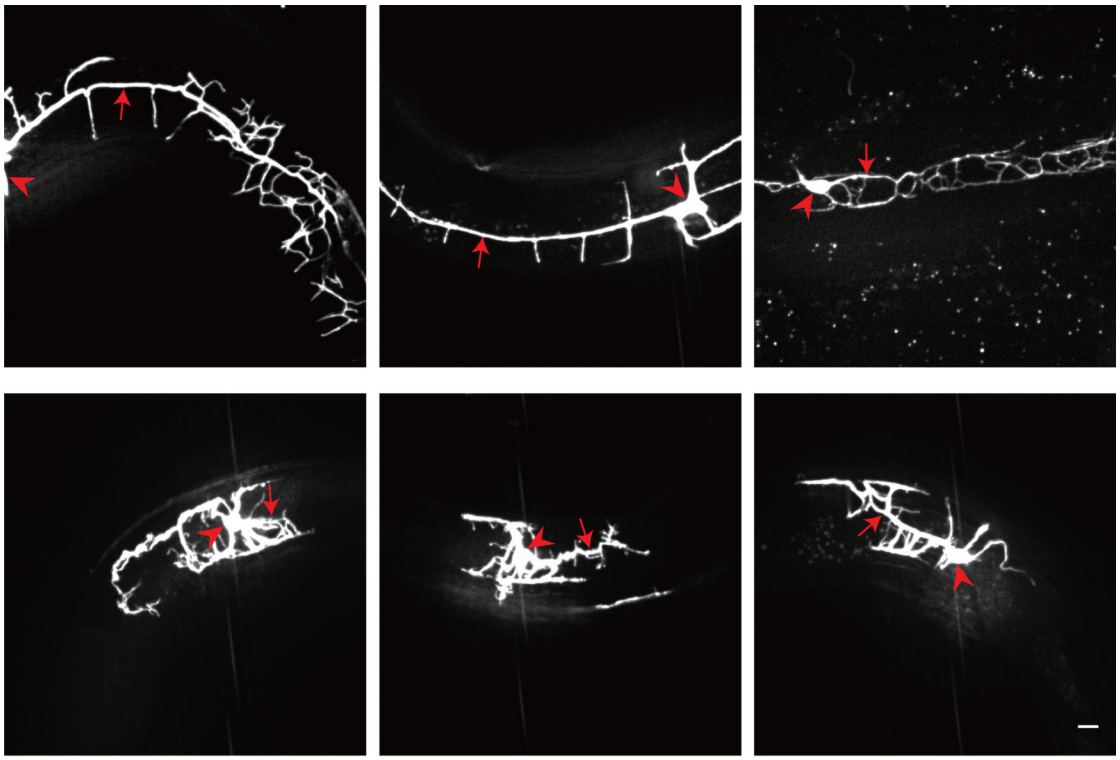

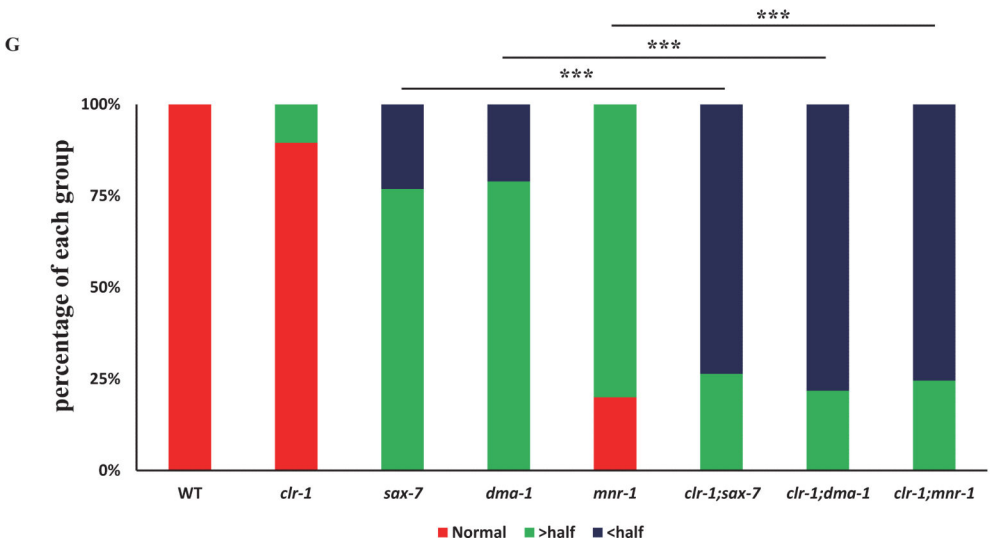

Fig. 5. *clr-1* functions redundantly with the SAX-7/MNR-1 pathway to control PVD 1° branch extension

A-F) Confocal images of young adult mutant animals expressing *ser-2*Prom3::GFP. Red arrows indicate the primary dendrites and red arrowheads point to cell bodies. Scale bar is 10μm. G) Quantification of primary dendrite length in wild type and different mutant backgrounds. "> half" means the length is greater than a half of a normal length of a PVD primary dendrite. "< half" means the length is less than a half of a normal length of a PVD primary dendrite. ***p < 0.001 by Chi-square test for multiple samples. n>30 for each genotype.

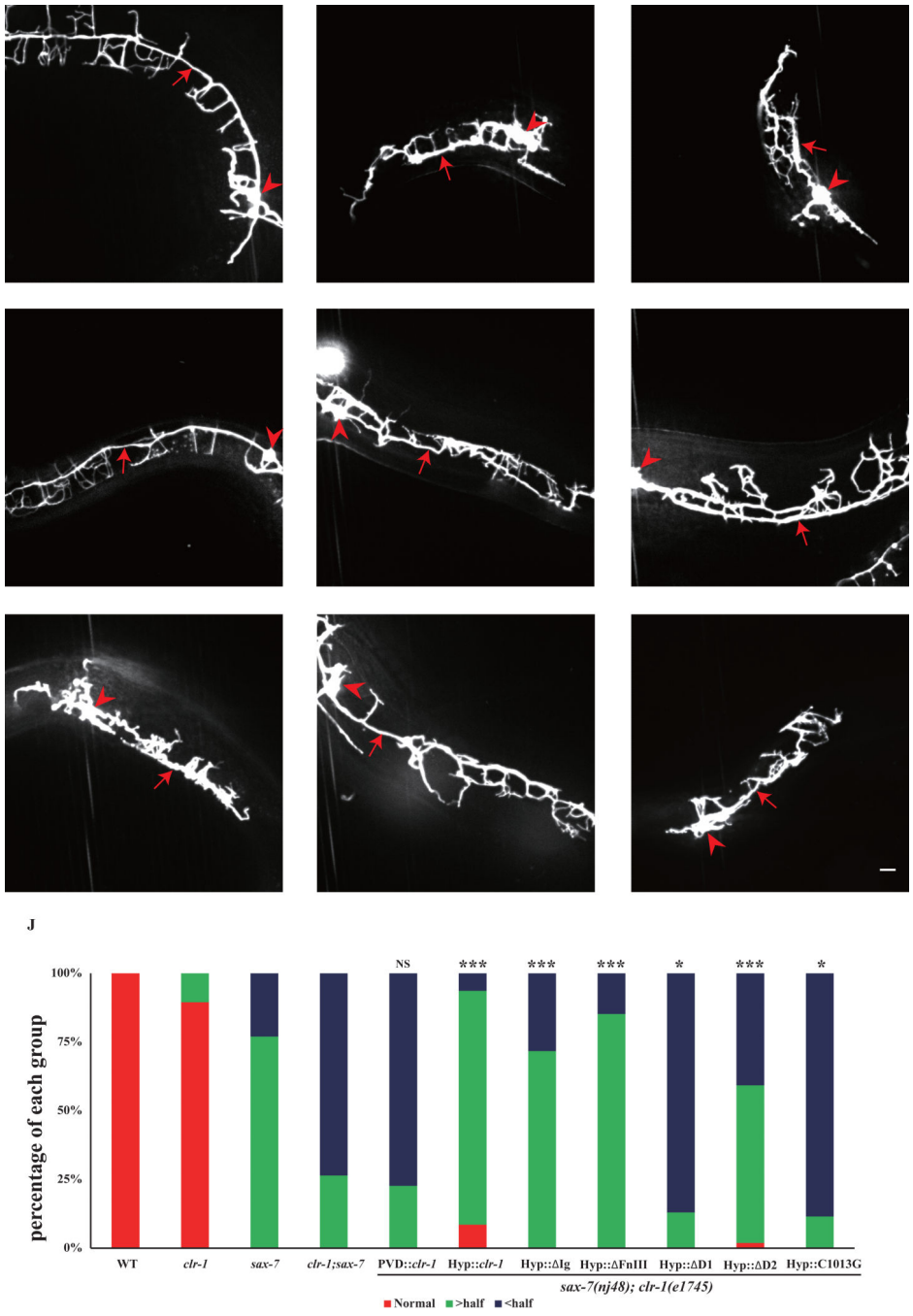

Fig. 6. *clr-1*'s function in PVD 1° dendrite extension is dependent on the intracellular phosphatase D1 domain

A-I) Confocal images of young adult mutant animals expressing *ser-2*Prom3::GFP. Red arrows indicate the primary dendrites and red arrowheads points to cell bodies. Scale bar is 10μm. J) Quantification of the rescuing activity of various constructs in *sax-7*(*nj48*); *clr-1*(*e1745ts*) mutation background. "> half" means the length is greater than a half of a normal length of a PVD primary dendrite. "< half" means the length is less than a half of a

normal length of a PVD primary dendrite. *p < 0.05, ***p < 0.001 by Chi-square test for multiple samples. n>30 for each genotype.